CHEMISTRY
A EUROPEAN JOURNAL

ChemPubSoc Europe

DOI: 10.1002/chem.201201468

Turn-On Fluorescence Sensor Based on Single-Walled-Carbon-Nanohorn–Peptide Complex for the Detection of Thrombin

Shuyun Zhu,[a, b, c] Zhongyuan Liu,[a] Lianzhe Hu,[a, c] Yali Yuan,[a, c] and Guobao Xu*[a]

Abstract: Proteases play a central role in several widespread diseases. Thus, there is a great need for the fast and sensitive detection of various proteolytic enzymes. Herein, we have developed a carbon nanotube (CNT)-based protease biosensing platform that uses peptides as a fluorescence probe for the first time. Single-walled carbon nanohorns (SWCNHs) and thrombin were used to demonstrate this detection strategy. SWCNHs can adsorb a fluorescein-based dye (FAM)-labeled peptide (FAM-pep) and quench the fluorescence of FAM. In contrast, thrombin can cleave FAM-pep on SWCNHs and recover the fluorescence of FAM, which allows the sensitive detection of thrombin. This biosensor has a high sensitivity and selectivity toward thrombin, with a detection limit of 100 pM.

Keywords: fluorescence · nanohorns · nanotubes · peptides · protease

Introduction

Proteases are important physiological enzymes that catalyze the hydrolysis of peptide bonds at specific sites and are widely used in analytical science today.[1–3] Bioinformatics data have revealed that proteases comprise nearly 2% of the human proteome.[4] Furthermore, proteases are abundant in almost every organism and they play key roles in a multitude of physiological reactions, from the simple digestion of food proteins to highly regulated cascades.[5,6] Misregulated proteolytic enzymes are associated with several widespread diseases, including cancers, degenerative diseases, coagulopathies, inflammation, and infectious diseases.[5,7] Various techniques have been reported for protease detection, such as calorimetry,[8] electrochemical methods,[9,10] and fluorescence.[11–14] Owing to their high sensitivity and operation convenience, fluorescence-based homogeneous assays are the most-popular methods for protease detection. These fluorescent assays generally rely on fluorescence resonance energy transfer (FRET). However, they usually require peptide-based molecular probes that contain both a fluorochrome and a quencher. The introduction of nanoquenchers can eliminate the selection issue of a fluorophore/quencher pair, avoid the labeling of the quencher, and thus save cost.

Thrombin, which is a serine protease, is a main effector protease of the tightly coordinated coagulation cascade. Thrombin generation is closely regulated to achieve rapid hemostasis after an injury.[15] However, inappropriate thrombin activity can activate platelets, monocytes, and the vascular endothelium to facilitate the formation of thrombi.[16] Furthermore, thrombosis is an important pathophysiologic component of many cardiovascular diseases. Thrombin can also promote tumor progression[17] and metastasis and it has been increasingly proposed as an important biomarker of deregulated programmed cell-death.[18] Thus, the detection of thrombin activity is of great significance in diagnostics and offers further insight into thrombin regulation.

Single-walled carbon nanohorns (SWCNHs) are horn-shaped carbon nanotubes (CNTs). Their diameters range from 2–5 nm and their length is about 40–50 nm. They typically assemble to form dahlia-like aggregates with a diameter of about 100 nm.[19] SWCNHs are prepared by vaporizing pure graphite rods by CO_2-laser ablation in Ar at ambient temperature without using any metal catalysts. SWCNHs are intrinsically free of metal contamination and pure SWCNHs can be produced cost-effectively. In contrast, pure single-walled CNTs are very expensive. Moreover, the horn-shaped structure of a single SWCNH and the dahlia-like structure of SWCNH aggregates offer SWCNHs many unique properties. As a result, SWCNHs have been widely used for various applications, such as adsorption, fuel cells, super capacitors, biosensors, and so on.[20–27] For example, SWCNHs has been used to construct a thrombin aptasensor with high sensitivity because SWCNHs have a high quenching efficiency toward FAM-labeled thrombin aptamer and the formation of a FAM-labeled thrombin-aptamer/thrombin complex can significantly increase fluorescence intensity.[28]

[a] S. Zhu, Z. Liu, L. Hu, Y. Yuan, Prof. G. Xu
State Key Laboratory of Electroanalytical Chemistry
Changchun Institute of Applied Chemistry
Chinese Academy of Sciences Changchun
Jilin 130022 (P.R. China)
Fax: (+86) 431-85262747
E-mail: guobaoxu@ciac.jl.cn

[b] S. Zhu
Shandong Provincial Key Laboratory of Life-Organic Analysis
College of Chemistry and Chemical Engineering
Qufu Normal University
Qufu, Shandong 273165 (P.R. China)

[c] S. Zhu, L. Hu, Y. Yuan
Graduate University of the Chinese Academy of Sciences
Chinese Academy of Sciences Changchun
Beijing 100039 (P.R. China)

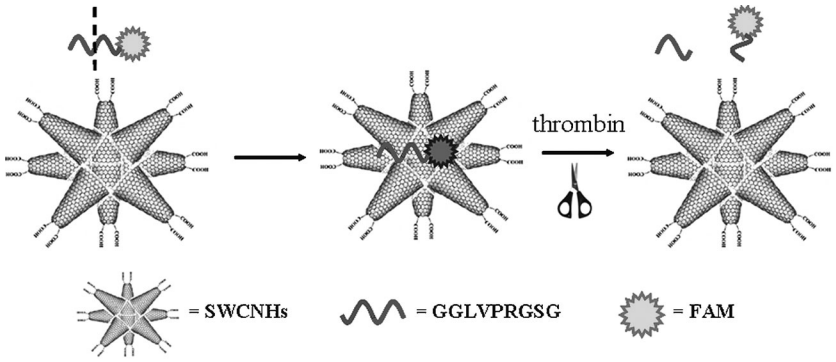

Scheme 1. Schematic illustration of the SWCNH–peptide fluorescence sensor for the detection of thrombin.

Herein, a CNT-based biosensor for protease that uses peptide as a fluorescence probe has been reported for the first time. As unique CNTs with the above-mentioned advantages, SWCNHs were used to test the feasibility of our design. Thrombin was used as a model protease. The principle of this biosensor is shown in Scheme 1. SWCNHs are added into a fluorescein-based dye (FAM)-labeled peptide (FAM-pep) solution to form the SWCNH–peptide complex. The fluorescence of FAM is quenched by SWCNHs owing to the proximity of FAM to SWCNHs. FAM-pep contains the core substrate (LVPRG) of thrombin. Therefore, thrombin can cleave FAM-pep and it weakens the interactions between FAM and SWCNHs, thereby resulting in the recovery of the fluorescence. This biosensor can detect 100 pM of thrombin with good selectivity.

Results and Discussion

Characterization of carboxylic-group-functionalized SWCNHs: To improve their dispersibility, the SWCNHs were first treated with a dilute solution of HNO_3 to obtain carboxylic-group-functionalized SWCNHs. Figure 1 shows a HRTEM image of carboxylic-group-functionalized SWCNHs; the functionalized SWCNHs maintain a dahlia-like morphology.[29] Figure 2 shows Raman spectra of the as-grown SWCNHs and carboxylic-group-functionalized SWCNHs. Both of these materials have two bands: a G band and a D band. The G band is related to the vibration mode in graphite-like carbon, whereas the D band is induced by disorder or edges within the structure.[30] The Raman spectrum of the as-grown SWCNHs show two broad peaks centered at 1340 cm^{-1} (D band) and 1568 cm^{-1} (G band) with similar intensities, which is characteristic of dahlia-shaped SWCNHs.[31] For carboxylic-group-functionalized SWCNHs, the intensity of the D band increases with the respect to that of the G band, which should be attributed to an increase in defect concentration on the walls of the nanohorn during acid treatment. In addition, the D- and G bands of the carboxylic-group-functionalized SWCNHs are up-shifted significantly by about 17 and 37 cm^{-1}, respectively, compared with those of as-grown SWCNHs. These result should be related to charge transfer between the SWCNHs and an electron acceptor (NO_2^+) that is formed by the decomposition of HNO_3.[31,32] The FTIR spectra of both as-grown SWCNHs and carboxylic-group-functionalized SWCNHs are shown in Figure 3. The peaks

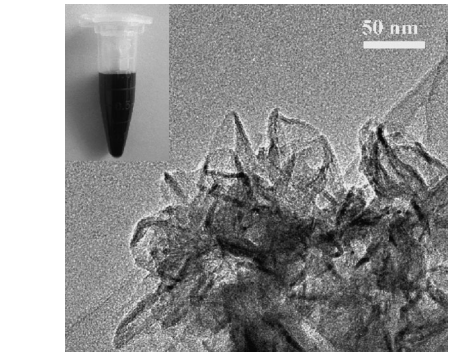

Figure 1. HRTEM images of carboxylic-group-functionalized SWCNHs. Inset: photograph of a 0.5 mg mL^{-1} aqueous solution of carboxylic-group-functionalized SWCNHs.

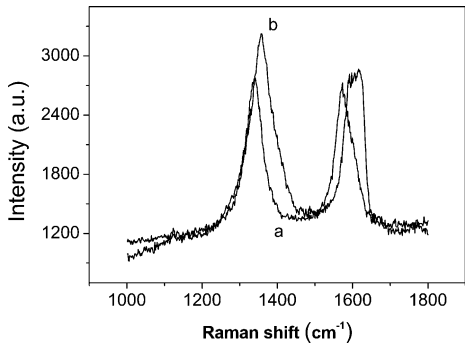

Figure 2. Raman spectra of a) as-grown SWCNHs and b) carboxylic-group-functionalized SWCNHs.

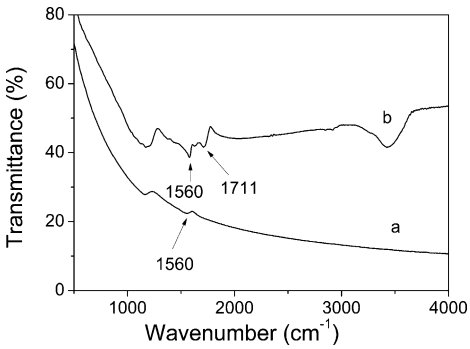

Figure 3. FTIR spectra of a) as-grown SWCNHs and b) carboxylic-group-functionalized SWCNHs.

at about 1560 cm^{-1} in both spectra were assigned to the C=C stretching mode that was associated with sidewall defects in the SWCNHs. The line at 1711 cm^{-1} was clearly assigned to the C=O stretching mode in the carboxylic-group-functionalized SWCNHs and indicated the generation of COOH groups.[33] Raman and FTIR spectroscopy and TEM data suggest that acid treatment leads to the formation of defects and COOH groups on the SWCNHs without destruction of the structure. The zeta potential of carboxylic-group-functionalized SWCNHs is about −60.5 mV, thus indicating that carboxylic-group-functionalized SWCNHs have a negatively charged surface, which may be due to the presence of COOH groups. So, there are electrostatic repulsion interactions among negatively charged carboxylic-group-functionalized SWCNHs, which contribute to the good dispersibility of SWCNHs in water.

Interactions of SWCNHs with FAM-pep and a possible mechanism: Figure 4 shows the fluorescence emission spectra of 150 nM FAM-pep under different conditions. FAM-pep exhibits strong fluorescence emission owing to the presence of FAM (Figure 4, curve a) and its quantum yield (QY) is 0.90 versus Rhodamine 6G as a standard (QY = 0.94). After the addition of 10.0 $\mu g mL^{-1}$ SWCNHs into a solution of FAM-pep, about 85% of the fluorescence is immediately quenched (Figure 4, curve b). Upon its incubation with 100 nM thrombin for only 1 min, the solution exhibits significant fluorescence enhancement, thereby leading to 45% fluorescence recovery (Figure 4, curve c). Note that both a solution of thrombin (Figure 4, curve d) and the mixed solution of thrombin and the SWCNHs (Figure 4, curve e) do not show any obvious fluorescence under the same experimental conditions. Thus, the increase in the intensity of the signal from curve b to curve c is due to the reaction of FAM-pep with thrombin and not from the autofluorescence of thrombin. The SWCNH sample has background fluorescence (Figure 4, curve f). Therefore, a background subtraction was performed for all of the SWCNH-involved measurements.

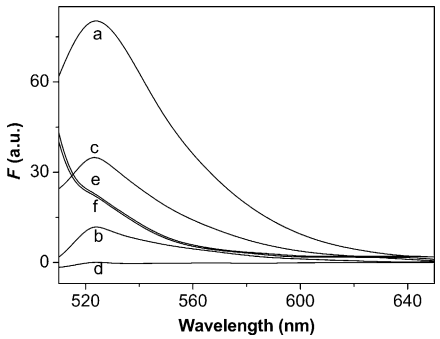

Figure 4. Fluorescence emission spectra of a) 150 nM FAM-pep, b) 150 nM FAM-pep+10.0 $\mu g mL^{-1}$ SWCNHs, c) 150 nM FAM-pep+10.0 $\mu g mL^{-1}$ SWCNHs+100 nM thrombin, d) 100 nM thrombin, e) 100 nM thrombin+10.0 $\mu g mL^{-1}$ SWCNHs, and f) 10.0 $\mu g mL^{-1}$ SWCNHs.

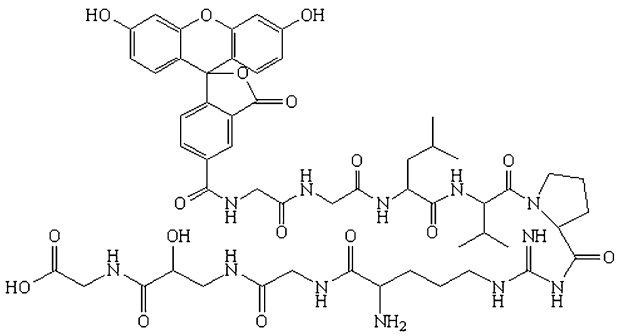

Scheme 2. Structure of FAM-pep.

The PI of FAM-pep is 9.75, owing to the presence of the NH_2 group from Arg (Scheme 2), thus indicating that FAM-pep has a positively charged surface in pH 7.4 Tris-HCl buffer. Moreover, the carboxylic-group-functionalized SWCNHs have a negatively charged surface. Thus, electrostatic interactions between the SWCNHs and FAM-pep may be a driving force that brings FAM into close proximity to the SWCNHs, thereby leading to quenching of the fluorescence. In contrast, thrombin can cleave the FAM-pep into two smaller parts. Thus, the interactions between FAM-pep and SWCNHs are weakened and, accordingly, it results in recovery of the fluorescence. To check whether this quenching phenomenon is attributed to the formation of the SWCNH–peptide complex or to simple collisions, we studied the effect of centrifugation on the fluorescence intensities. Figure 5a,b shows that centrifugation has essentially no effect on the fluorescence intensity of the FAM-pep solution, thus indicating that FAM-pep is not removed by centrifugation. Most of fluorescence is quenched after the addition of SWCNHs (Figure 5c). After the mixed solution of FAM-pep and SWCNHs is centrifuged, the supernatant shows much-weaker fluorescence (Figure 5d) compared to that of the FAM-pep solution. This result demonstrates that FAM-pep adsorbs onto SWCNHs and is mostly removed by centrifugation through the formation of the SWCNH–pep-

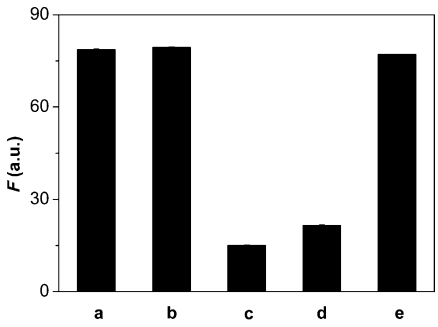

Figure 5. Fluorescence intensities of a) 150 nM FAM-pep solution, b) the supernatant of (a) after centrifugation, c) a mixed solution of 150 nM FAM-pep+10.0 $\mu g mL^{-1}$ SWCNHs, d) the supernatant of (c) after centrifugation, and e) the supernatant of a mixed solution of 150 nM FAM-pep+10.0 $\mu g mL^{-1}$ SWCNHs+100 nM thrombin after centrifugation.

tide complex. The supernatant shows slightly stronger fluorescence than the mixed solution of FAM-pep and SWCNHs. This increase is probably because the SWCNH–peptide complex cannot be totally removed by centrifugation and/or simple collisions may play some role in the quenching of the fluorescence. In contrast, after centrifugation, the supernatant of the mixed solution of FAM-pep, SWCNHs, and thrombin (Figure 5e) has almost the same fluorescence intensity as the FAM-pep solution. These results indicate that thrombin can cleave FAM-pep and that the resulting fragment of FAM-pep cannot adsorb onto the SWCNHs.

Optimization of the amount of SWCNHs: Next, the optimal amount of SWCNHs as a nanoquencher for FAM-pep was determined. As shown in Figure 6, the fluorescence of

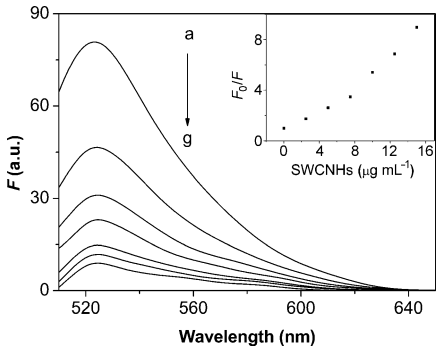

Figure 6. Fluorescence spectra of FAM-pep (150 nM) in the presence of various concentrations of SWCNHs: a) 0, b) 2.5, c) 5.0, d) 7.5, e) 10.0, f) 12.5, and g) 15.0 μg mL^{-1}. Inset: variation in the fluorescence-intensity ratios (F_0/F) at 522 nm versus the concentration of SWCNHs, where F_0 and F are the fluorescence intensity of FAM-pep before and after the addition of SWCNHs, respectively.

FAM-pep decreases gradually with an increase in the concentration of SWCNHs. The corresponding Stern–Volmer plot (Figure 6, inset) displays an upward-curving shape, thus suggesting the formation of a static SWCNH–peptide complex. The fluorescence-intensity ratio (F_0/F), where F_0 and F are the fluorescence intensities of FAM-pep before and after the addition of SWCNHs, respectively, increases from 1.74 at a SWCNH concentration of 2.5 μg mL^{-1} to 8.97 at a concentration of 15.0 μg mL^{-1}. An increase in the concentration of SWCNHs leads to an increase in quenching efficiency but a decrease in fluorescence recovery. Therefore, we used a concentration of 10.0 μg mL^{-1} in the following experiments.

Effect of time: The effect of incubation time on fluorescence intensity was also investigated by collecting time-independent fluorescence emission spectra. As shown in Figure 7, curve a, in the absence of thrombin, there is a rapid drop in intensity in the first 1 min and then a slight decrease over the following 59 min. The fluorescence quench-

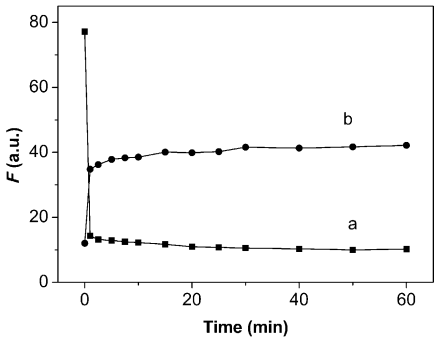

Figure 7. a) Fluorescence quenching of 150 nM FAM-pep by 10.0 μg mL^{-1} SWCNHs and b) fluorescence recovery of a SWCNH–peptide complex by 100 nM thrombin as a function of incubation time.

ing of FAM-pep by SWCNHs is a very quick process and more than 80% of the fluorescence is quenched after the addition of SWCNHs for 1 min. After the addition of thrombin to the SWCNH–peptide complex, the fluorescence signal increases quickly within the first 1 min and then slowly thereafter (Figure 7, curve b). Up to 45% of the fluorescence is recovered after the addition of thrombin for 1 min. Both fluorescence quenching and fluorescence recovery are very fast. Therefore, reaction times of 1 min for fluorescence quenching and -recovery were used, respectively.

Detection of thrombin: Figure 8 shows the fluorescence emission spectra of a SWCNH–peptide complex upon incubation with various concentrations of thrombin in the range 0–200 nM. Figure 8, inset shows a plot of the change in fluorescence intensity (ΔF) versus the concentrations of thrombin. The fluorescence intensities of the SWCNH–peptide complex increased with increasing concentration of thrombin. A detection limit of 100 pM was achieved with this sensor, which is 20-fold better than that of the fluorescence sensor that was based on graphene oxide, (GO)–peptide.[34] Moreover, the synthesis of GO generally involves toxic and/or corrosive materials and tedious procedures. Moreover,

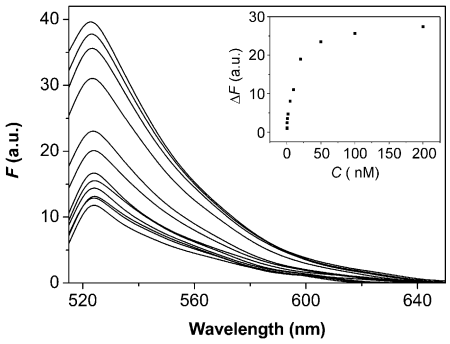

Figure 8. Fluorescence spectra of the SWCNH–peptide complex in the presence of various concentrations of thrombin. From bottom to top: 0.0, 0.1, 0.2, 0.5, 1.0, 2.0, 5.0, 10.0, 20.0, 50.0, 100.0, 200.0 nM. Inset plot of ΔF versus the concentration of thrombin; ΔF is the difference in fluorescence intensity of the SWCNH–peptide complex in the presence and absence of thrombin.

Table 1. Comparison of different methods for the detection of thrombin.

Method	Probe	Assay time	Detection limit	Reference
label-free electronic aptasensor	Methylene blue-aptamer	19 h	6.4 nM	[35]
chemiluminescence aptasensor	DNAzyme	27 h	0.1 nM	[36]
aptamer-based colorimetric sensor	AuNPs	5 min	0.83 nM	[37]
fluorescence aptasensor	Ag nanoclusters	55 min	1 nM	[38]
graphene oxide (GO)-based fluorescence aptasensor	FAM-aptamer	35 min	2 nM	[35]
SWCNH-based fluorescence aptasensor	FAM-aptamer	11 min	100 pM	[28]
SWCNT-based fluorescence aptasensor	FAM-aptamer	2–3 h	1.8 nM	[40]
amplified fluorescence aptasensor	dye-thrombin aptamer	12 min	89 pM	[41]
fluorescence sensor based on a GO–peptide complex	FAM-peptide	5 min	2 nM	[34]
fluorescence sensor based on a SWCNH–peptide complex	FAM-peptide	2 min	100 pM	this work

GO is unstable and its properties readily change during storage. In contrast, SWCNHs are prepared with high purity by vaporizing pure graphite rods through CO_2-laser ablation under an Ar atmosphere at ambient temperature. These SWCNHs are very stable and, thus, are more user-friendly. Compared with the other reported methods, our method has a comparable-or-better detection limit (Table 1). In addition, our method is very time-saving. The whole assay can be finished within several minutes. The fluorescence sensor has good reproducibility with relative standard deviations of less than 5%.

Selectivity of thrombin detection: To confirm that the recovery of fluorescence was caused by thrombin, we investigated the selectivity of this fluorescence sensor. Figure 9 shows the ΔF values when this sensor was incubated separately with 100 nM of thrombin, bovine serum albumin (BSA), human IgG, trypsin, papain, glucose oxidase (GOx), and myoglobin. The sensor showed a significant increase in fluorescence for thrombin, whilst it showed a weak response to other proteases or proteins. This result indicates that our present fluorescence sensor exhibits good selectivity toward thrombin.

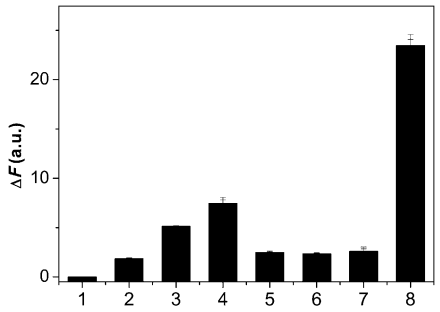

Figure 9. Changes in the fluorescence intensity of the sensor incubated in a) blank buffer and buffer that contains 100 nM of b) BSA, c) human IgG, d) trypsin, e) papain, f) GOx, g) myoglobin, and h) thrombin; [FAM-pep] = 150 nM, [SWCNHs] = 10.0 $\mu g\,mL^{-1}$.

Conclusion

In conclusion, SWCNHs, as a unique type of CNTs, have been developed as a new biosensing platform that uses peptides as a probe for the first time. This biosensing platform has been applied to sensitively and selectively detect thrombin down to the pM level because of the exceptionally high fluorescence-quenching efficiency of SWCNHs. Moreover, SWCNHs can act as a common nanoquencher for different kinds of fluorescent dyes. Thus, this platform is promising for the multiplexed detection of different proteases.

Experimental Section

Materials: Professor S. Iijima generously offered SWCNHs that were prepared at RT by CO_2-laser ablation. The FAM-labeled peptide (FAM-GGLVPRGSG, FAM-pep) was synthesized by GL Biochem (Shanghai) Ltd. Thrombin, trypsin, myoglobin, and GOx were bought from Sigma (U.S.A.). Bovine serum albumin (BSA) and human IgG antibody were bought from Dingguo Biotech. (Beijing, China). Papain was purchased from Sangon Biotech Co. Ltd.

Apparatus: HRTEM measurements were performed on a FEI TECNAI G2 F20 microscope that was operated at an accelerating voltage of 200 kV. Zeta-potential measurements were performed on a Zetasizer Nano-ZS 90 (Malver Instruments Ltd., U.K.). Fourier-transform IR (FTIR) spectroscopy experiment was operated on a BRUKER Vertex 70 FTIR spectrometer (Germany). Raman spectra were recorded on a Renishaw system 2000 Raman spectrometer that was operated with an Ar^+-ion laser (514.5 nm). Fluorescence measurements were performed on a Perkin–Elmer LS55 Luminescence Spectrometer (Perkin–Elmer Instruments, U.K.).

Preparation of carboxylic-group-functionalized SWCNHs: Carboxylic-group-functionalized SWCNHs were prepared as follows: SWCNHs were dispersed in 30% HNO_3 and then heated at reflux (140 °C) for 24 h to obtain carboxylic-group-functionalized SWCNHs. The resulting suspension was centrifuged and the sediment was washed with doubly distilled water until the pH value reached 6.0. The oxidized SWCNHs were dried at 60 °C overnight and then dispersed in doubly distilled water to form a stable suspension with a concentration of 0.5 $mg\,mL^{-1}$.

Analytical procedures: In a typical measurement, an aliquot of a freshly made suspension of SWCNHs was added to 150 nM FAM-pep in 20 mM Tris-HCl buffer (pH 7.42, with 50 mM NaCl, 5 mM KCl, and 5 mM $MgCl_2$ to incubate for 1 min. Then, a different concentration of thrombin was added to the above mixture. After incubation for 1 min, fluorescence measurements were recorded. The fluorescence was monitored at 522 nm with excitation at 480 nm at RT.

Acknowledgements

The authors are very grateful to Prof. S. Iijima (Solution Oriented Research for Science and Technology, Japan Science and Technology Agency) for the generous offer of SWCNHs. This work was kindly sup-

ported by the National Natural Science Foundation of China (Nos 21175126 and 20875086).

[1] B. Turk, *Nat. Rev. Drug Discovery* **2006**, *5*, 785–799.
[2] K. Mann, M. Mann, *Proteomics* **2008**, *8*, 178–191.
[3] X. Zhang, A. Fang, C. P. Riley, M. Wang, F. E. Regnier, C. Buck, *Anal. Chim. Acta* **2010**, *664*, 101–113.
[4] N. D. Rawlings, D. P. Tolle, A. J. Barret, *Nucleic Acids Res.* **2004**, *32*, D160–164.
[5] M. Drag, G. S. Salvesen, *Nat. Rev. Drug Discovery* **2010**, *9*, 690–701.
[6] N. D. Rawlings, A. J. Barret, A. Bateman, *Nucleic Acids Res.* **2010**, *38*, D227–233.
[7] R. B. Lefkowitz, G. W. Schmid-Schonbein, M. J. Heller, *Anal. Chem.* **2010**, *82*, 8251–8258.
[8] C. Guarise, L. Pasquato, V. De Filippis, P. Scrimin, *Proc. Natl. Acad. Sci. USA* **2006**, *103*, 3978–3982.
[9] B. A. Zaccheo, R. M. Crooks, *Anal. Chem.* **2011**, *83*, 1185–1188.
[10] K. A. Mahmoud, J. H. T. Luong, *Anal. Chem.* **2008**, *80*, 7056–7062.
[11] X. H. Wang, J. Geng, D. Miyoshi, J. S. Ren, N. Sugimoto, X. Q. Qu, *Biosens. Bioelectron.* **2010**, *26*, 743–747.
[12] Y. Wang, Y. Zhang, B. Liu, *Anal. Chem.* **2010**, *82*, 8604–8610.
[13] Q. Zhu, R. Zhan, B. Liu, *Macromol. Rapid Commun.* **2010**, *31*, 1060–1064.
[14] L. An, L. Liu, S. Wang, *Biomacromolecules* **2009**, *10*, 454–457.
[15] J. T. B. Crawley, S. Zanardelli, C. K. N. K. Chion, D. A. Lane, *J. Thromb. Haemostasis* **2007**, *5*, 95–101.
[16] S. R. Coughlin, *Nature* **2000**, *407*, 258–264.
[17] M. E. Maragoudakis, N. E. Tsopanoglou, P. Andriopoulou, M. M. Maragoudakis, *Matrix Biol.* **2000**, *19*, 345–351.
[18] K. L. Moffitt, S. L. Martin, B. Walker, *Biochem. Soc. Trans.* **2007**, *35*, 559–560.
[19] S. Iijima, M. Yudasaka, R. Yamada, S. Bandow, K. Suenaga, F. Kokai, K. Takahashi, *Chem. Phys. Lett.* **1999**, *309*, 165–170.
[20] E. Bekyarova, K. Murata, M. Yudasaka, D. Kasuya, S. Iijima, H. Tanaka, H. Kanoh, K. Kaneko, *J. Phys. Chem. B* **2003**, *107*, 4681–4684.
[21] D. Tasis, N. Tagmatarchis, V. Georgakilas, M. Prato, *Chem. Eur. J.* **2003**, *9*, 4001–4008.
[22] C. M. Yang, Y. J. Kim, M. Endo, H. Kanoh, M. Yudasaka, S. Iijima, K. Kaneko, *J. Am. Chem. Soc.* **2007**, *129*, 20–21.
[23] S. Y. Zhu, G. B. Xu, *Nanoscale* **2010**, *2*, 2538–2549.
[24] G. Mountrichas, S. Pispas, T. Ichihasi, M. Yudasaka, S. Iijima, N. Tagmatarchis, *Chem. Eur. J.* **2010**, *16*, 5927–5933.
[25] J. Miyawaki, M. Yudasaka, T. Azami, Y. Kubo, S. Iijima, *ACS NANO* **2008**, *2*, 213–226.
[26] J. Miyawaki, S. Matsumura, R. Yuge, T. Murakami, S. Sato, A. Tomida, T. Tsuruo, T. Ichihashi, T. Fujinmi, H. Irie, K. Tsuchida, S. Iijima, K. Shiba, M. Yudasaka, *ACS NANO* **2009**, *3*, 1399–1406.
[27] S. Y. Zhu, Z. Y. Liu, W. Zhang, S. Han, L. Z. Hu, G. B. Xu, *Chem. Commun.* **2011**, *47*, 6099–6101.
[28] S. Y. Zhu, S. Han, L. Zhang, S. Parveen, G. B. Xu, *Nanoscale* **2011**, *3*, 4589–4592.
[29] C. M. Yang, H. Noguchi, K. Murata, M. Yudasaka, A. Hashimoto, S. Iijima, K. Kaneko, *Adv. Mater.* **2005**, *17*, 866–870.
[30] M. Terrones, A. R. Botello-Méndez, J. Campos-Delgado, F. López-Urías, Y. I. Vega-Cantú, F. J. Rodríguez-Macías, A. L. Elías, E. Muñoz-Sandoval, A. G. Cano-Márquez, J. C. Charlier, H. Terrones, *Nano Today* **2010**, *5*, 351–372.
[31] S. Bandow, A. M. Rao, G. U. Sumanasekera, P. C. Eklund, F. Kokai, K. Takahashi, M. Yudasaka, S. Iijima, *Appl. Phys. A* **2000**, *71*, 561–564.
[32] A. M. Rao, P. C. Eklund, S. Bandow, A. Thess, R. E. Smalley, *Nature* **1997**, *388*, 257–259.
[33] Y. B. Wang, Z. Iqbal, S. Mitra, *Carbon* **2005**, *43*, 1015–1020.
[34] M. Zhang, B. C. Yin, X. F. Wang, B. C. Ye, *Chem. Commun.* **2011**, *47*, 2399–2401.
[35] Y. Xiao, A. A. Lubin, A. J. Heeger, K. W. Plaxco, *Angew. Chem.* **2005**, *117*, 5592–5595; *Angew. Chem. Int. Ed.* **2005**, *44*, 5456–5459.
[36] T. Li, E. K. Wang, S. J. Dong, *Chem. Commun.* **2008**, 5520–5522.
[37] H. Wei, B. L. Li, E. K. Wank, S. J. Dong, *Chem. Commun.* **2007**, 3735–3737.
[38] J. Sharma, H. C. Yeh, H. Yoo, J. H. Werner, J. S. Martinez, *Chem. Commun.* **2011**, *47*, 2294–2296.
[39] C. H. Lu, H. H. Yang, C. L. Zhu, X. Chen, G. N. Chen, *Angew. Chem.* **2009**, *121*, 4879–4881; *Angew. Chem. Int. Ed.* **2009**, *48*, 4785–4787.
[40] R. H. Yang, Z. W. Tang, J. L. Yan, H. Z. Kang, Y. M. Kin, Z. Zhu, W. H. Tan, *Anal. Chem.* **2008**, *80*, 7408–7413.
[41] X. Q. Liu, R. Freeman, I. Willner, *Chem. Eur. J.* **2012**, *18*, 2207–2211.

Received: April 28, 2012
Revised: July 23, 2012
Published online: October 4, 2012

